Received: 15 October 2023 | Revised: 4 January 2024 | Accepted: 19 January 2024

DOI: 10.1002/nme.7443

RESEARCH ARTICLE

WILEY

Transverse shear parametrization in hierarchic large rotation shell formulations

Rebecca Thierer[1] | **Bastian Oesterle**[2] | **Ekkehard Ramm**[1] | **Manfred Bischoff**[1]

[1]University of Stuttgart, Institute for Structural Mechanics, Stuttgart, Germany

[2]Hamburg University of Technology, Institute for Structural Analysis, Hamburg, Germany

Correspondence
Rebecca Thierer, University of Stuttgart, Institute for Structural Mechanics, Pfaffenwaldring 7, Stuttgart, 70550, Germany.
Email: thierer@ibb.uni-stuttgart.de

Funding information
Deutsche Forschungsgemeinschaft, Grant/Award Number: 428725889

Abstract

Consistent treatment of large rotations in common Reissner–Mindlin formulations is a complicated task. Reissner–Mindlin formulations that use a hierarchic parametrization provide an elegant way to facilitate large rotation shell analyses. This can be achieved by the assumption of linearized transverse shear strains, resulting in an additive split of strain components, which technically simplifies implementation of corresponding shell finite elements. The present study aims at validating this assumption by systematically comparing numerical solutions with those of a newly implemented hierarchic and fully nonlinear Reissner–Mindlin shell element.

KEYWORDS

hierarchic shell formulation, isogeometric analysis, large rotations, linearized transverse shear, Reissner–Mindlin model, shear deformable shells

1 | INTRODUCTION

Plate and shell models including the effect of transverse shear deformation are commonly referred to as *Reissner–Mindlin models*. This gives credit to the pioneering contributions of Eric Reissner[1] and Raymond D. Mindlin,[2] who were among the first to explicitly address the effect of transverse shear deformation on the mechanical behavior of plates in bending. Strictly speaking, there is no such thing as a unique Reissner–Mindlin *theory*, because both formulations differ in technical details. Nevertheless, the terms Reissner–Mindlin *model* and Reissner–Mindlin *kinematics* seem to be justified and they are widely accepted. As an alternative, the term *first order shear deformation theory* is frequently used. The extension of the originally linear models to geometrically nonlinear problems is often associated with the name of *Naghdi*,[3] particularly in the mathematical community. Today, geometrically (and materially) nonlinear analyses of shells using the Reissner–Mindlin model are commonplace in both science and industry.

One of the reasons for the success of the concept is the fact that in the context of the finite element method as a solution scheme C^0-continuous shape functions are sufficient, while the Kirchhoff–Love "thin" shell model,[4,5] or the *Koiter shell model*[6] in its nonlinear version, requires C^1-continuity. The notorious problem of transverse shear locking, coming along with the independent parametrization of rotations of the shell director and displacements of the mid-surface, is a drawback of shear deformation theories in comparison to the shear rigid Kirchhoff–Love model. However, in the meantime various methods are available to alleviate it, for example, reduced integration,[7] assumed strains and mixed methods, see Zienkiewicz and Taylor[8] and Zienkiewicz, Taylor and Fox [9] for an overview.

Dedicated with great gratitude to Bob Taylor on the occasion of his 90th birthday for his inspiring contributions in structural mechanics and his friendship to two of us, based on fruitful cooperation in Berkeley and close personal relations over many years.

Nearly two decades ago, the introduction of *isogeometric analysis (IGA)* by Hughes et al.[10] triggered a renaissance of the Kirchhoff–Love model, because the usage of splines, particularly non-uniform rational b-splines (NURBS) promises an easier construction of C^1-continuous function spaces for discretization. Kiendl et al.[11] where the first to exploit this feature for a Kirchhoff–Love type IGA shell formulation.

Soon, however, it has been found that C^1-continuity can also be beneficial for the Reissner–Mindlin model. Long et al.[12] presented a shell formulation based on subdivision surfaces, in which the total rotation of the shell director is split into a contribution of the rotation of the surface normal and the transverse shear part. Before the development of IGA, the same group had already presented a Kirchhoff–Love shell formulation based on subdivision surfaces in Cirak et al.[13] as early as 2000. A concept similar to Long et al.[12] was developed in Echter et al.[14] for a hierarchic Reissner–Mindlin IGA shell formulation. Because derivatives of the displacement field are involved in the construction of the rotated normal, C^1-continuity is required for discretization.

As the transverse shear part is described by distinct degrees of freedom, these formulations are intrinsically free from transverse shear locking, without any additional measures. Indeed, a Kirchhoff–Love formulation can directly be extracted by simply constraining the transverse shear degrees of freedom to zero. This particular feature is shared by the mixed element formulation of Auricchio and Taylor.[15,16] Therein, the specific construction of the underlying multi-field functional allows to "switch off" the transverse shear part, thus combining the Reissner–Mindlin and the Kirchhoff–Love model in one unique hierarchic formulation. It has been extended to shells by Bischoff and Taylor.[17]

The formulation of Echter et al.[14] is limited to geometrically linear problems and uses a difference vector to represent the change of direction of the director related to transverse shear deformation. The components of this difference vector can be easily transformed into rotation angles and in fact this formulation is aptly characterized as a formulation with *hierarchic rotations*. As already mentioned, it is intrinsically free from transverse shear locking. However, if equal order interpolation is used for the mid-surface displacements and the components of the difference vector (a.k.a. hierarchic rotations) oscillations of the transverse shear forces can be observed.

Oesterle et al.[18] succeeded in overcoming this problem by proposing a completely rotation-free Reissner–Mindlin shell formulation, in which the hierarchic part, describing the shear deformation, is obtained from derivatives of additional displacement degrees of freedom that can be interpreted as "shear displacements." This still geometrically linear formulation is free from transverse shear locking and does not exhibit any oscillations. Henceforth, this type of model is denoted as formulation with *hierarchic displacements*.

Eventually, Oesterle et al.[19] presented geometrically nonlinear versions of the hierarchic rotation and hierarchic displacement formulations. They are capable of dealing with large rotations and large membrane and bending strains. The transverse shear part, however, is linear. In other words, total rotations can be large, but the shear angles are assumed to be small. The reasons for this restriction are mostly technical. In particular, it dramatically simplifies linearization, because there is an additive split of strains emanating from the bending and transverse shear parts. Unlike conventional nonlinear Reissner–Mindlin shell elements, this concept does not require to deal with rotation tensors and algorithms for large rotations.

Recently, Neunteufel and Schöberl[20] adopted the hierarchic rotation approach to enhance their previously presented nonlinear Kirchhoff–Love shell element by transverse shear strains to obtain a Reissner–Mindlin shell element. The formulation is based on the mixed Hellan–Herrmann–Johnson method with a focus on membrane locking.

Quite naturally, the question arises, whether the restriction to small transverse shear angles would compromise the predictive capabilities of the model in certain situations. It may well be possible that for relatively thick shells or very large gradients of bending moments or composite shells with a soft core, large shear angles and corresponding geometrically nonlinear effects are not negligible. Although this problem has already been mentioned to a certain extent,[19,21] it is the major motivation for the present study.

Interestingly, nonlinear Reissner–Mindlin shell elements with linearized shear rotations can also be encountered in commercial finite element software, although this is barely noted in the literature. The *Belytschko–Lin–Tsay element*[22] is one of the workhorses in the commercial code LS-DYNA[23] for explicit dynamic analyses, for instance in crash and metal forming simulations. As described in Belytschko et al.,[22] it uses the assumption that the angle between the director and the normal remains small. For the shear deformable shell element SHELL181 in ANSYS, the underlying mathematical formulation is not disclosed in the theory manual [24] and the authors are not aware of any detailed theoretical description of the element. The documentation indeed mentions that "SHELL181 includes the linear effects of transverse shear deformation."[24] A simple numerical experiment, applying prescribed nodal rotations, while fixing all other degrees of freedom, along with the option of a linear elastic material, reveals for both elements a linear relation between shear stress and rotation, regardless of the magnitude of the rotations.

The reasons or the motivation for these simplifications in commercial codes are, to the authors' knowledge, not named. It is, however, well known that consistent treatment of large rotations is an awkward task, because, unlike displacements, large rotations do not live in a linear vector space, see Zienkiewicz, Taylor and Fox [9] for a concise theoretical summary and Müller and Bischoff[25] for a recent contribution and an overview of the state of the art in this area. At least for the concept followed in LS-DYNA, it can be said that it successfully circumvents dealing with rotation tensors and corresponding update algorithms for large rotations.

The present study provides a systematic investigation of the effect of linearized transverse shear parametrization in the context of hierarchic shell elements by means of numerical experiments, devised to trigger potential nonlinear phenomena associated with (large) transverse shear deformations.

2 | TRANSVERSE SHEAR PARAMETRIZATION IN HIERARCHIC SHELL FORMULATIONS

2.1 | Differential geometry and shell kinematics

The presented shell formulations use a convective curvilinear coordinate system with in-plane coordinates ξ^α, which span the shell mid-surface, and a thickness coordinate $\xi^3 \in \left[-\frac{t}{2}, \frac{t}{2}\right]$ with shell thickness t. Greek indices take on values of 1 or 2, while Latin indices run from 1 to 3. Partial derivatives w.r.t. the curvilinear coordinates are written as $(\ )_{,i} = \frac{\partial(\ )}{\partial \xi^i}$. Quantities of the reference configuration are represented by capital letters, whereas small letters refer to the current configuration, compare Figure 1.

Using dimensional reduction and a total Lagrangian setting, the position of an arbitrary point of the shell body is described by its mid-surface position and the director:

$$\mathbf{X}(\xi^i) = \mathbf{R}(\xi^\alpha) + \xi^3 \mathbf{A}_3(\xi^\alpha), \quad \mathbf{x}(\xi^i) = \mathbf{r}(\xi^\alpha) + \xi^3 \mathbf{a}_3(\xi^\alpha). \tag{1}$$

The reference director $\mathbf{A}_3$ is defined as the normalized cross product of the in-plane covariant base vectors $\mathbf{A}_\alpha$:

$$\mathbf{A}_3 = \frac{\mathbf{A}_1 \times \mathbf{A}_2}{\|\mathbf{A}_1 \times \mathbf{A}_2\|} \text{ with } \mathbf{A}_\alpha = \mathbf{R}_{,\alpha}. \tag{2}$$

The definition of the current director $\mathbf{a}_3$ depends on the shell formulation and is given in Sections 2.2 and 2.3.

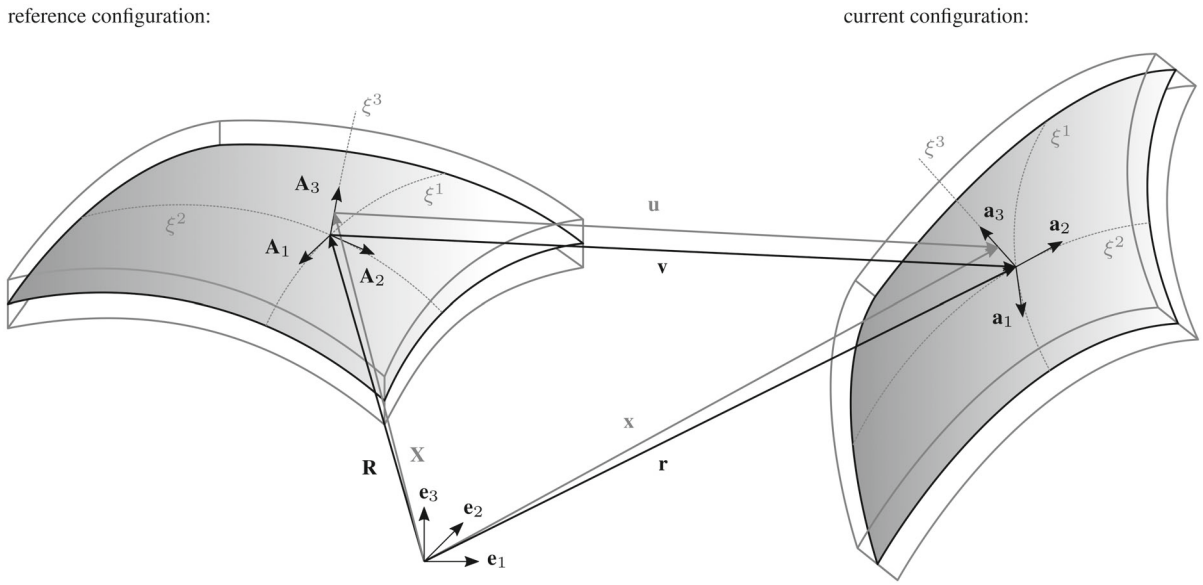

FIGURE 1 Shell body in reference configuration and current configuration.

Thus, the displacement field for a point of the shell body $\mathbf{u}$ is defined by the difference of position vectors in reference configuration and current configuration. With dimensional reduction, the deformation is split into mid-surface displacements $\mathbf{v}$ and the difference between directors:

$$\mathbf{u} = \mathbf{x} - \mathbf{X} = \mathbf{r} + \xi^3 \mathbf{a}_3 - \left(\mathbf{R} + \xi^3 \mathbf{A}_3\right) = \mathbf{v} + \xi^3(\mathbf{a}_3 - \mathbf{A}_3). \tag{3}$$

The three-dimensional Green–Lagrange strain tensor is defined as

$$\mathbf{E} = E_{ij}\mathbf{G}^i \otimes \mathbf{G}^j \text{ with } E_{ij} = \left(\mathbf{u}_{,i} \cdot \mathbf{G}_j + \mathbf{u}_{,j} \cdot \mathbf{G}_i + \mathbf{u}_{,i} \cdot \mathbf{u}_{,j}\right) \tag{4}$$

with the covariant base vectors of the shell body

$$\begin{aligned} \mathbf{G}_\alpha &= \mathbf{X}_{,\alpha} = \mathbf{R}_{,\alpha} + \xi^3 \mathbf{A}_{3,\alpha} = \mathbf{A}_\alpha + \xi^3 \mathbf{A}_{3,\alpha}, \\ \mathbf{G}_3 &= \mathbf{X}_{,3} = \mathbf{A}_3. \end{aligned} \tag{5}$$

Using Equation (3), utilizing orthogonality ($\mathbf{A}_\alpha \cdot \mathbf{A}_3 = 0$ and $\mathbf{a}_{3,\alpha} \cdot \mathbf{a}_3 = 0$), and neglecting terms quadratic in ξ^3, the strain components read

$$\begin{aligned} E_{11} &= \mathbf{v}_{,1} \cdot \mathbf{A}_1 + \frac{1}{2}\mathbf{v}_{,1} \cdot \mathbf{v}_{,1} + \xi^3\left(\mathbf{a}_1 \cdot \mathbf{a}_{3,1} - \mathbf{A}_1 \cdot \mathbf{A}_{3,1}\right), \\ 2E_{12} &= \mathbf{v}_{,1} \cdot \mathbf{A}_2 + \mathbf{v}_{,2} \cdot \mathbf{A}_1 + \mathbf{v}_{,1} \cdot \mathbf{v}_{,2} + \xi^3\left(\mathbf{a}_1 \cdot \mathbf{a}_{3,2} + \mathbf{a}_2 \cdot \mathbf{a}_{3,1} - \mathbf{A}_1 \cdot \mathbf{A}_{3,2} - \mathbf{A}_2 \cdot \mathbf{A}_{3,1}\right), \\ E_{22} &= \mathbf{v}_{,2} \cdot \mathbf{A}_2 + \frac{1}{2}\mathbf{v}_{,2} \cdot \mathbf{v}_{,2} + \xi^3\left(\mathbf{a}_2 \cdot \mathbf{a}_{3,2} - \mathbf{A}_2 \cdot \mathbf{A}_{3,2}\right), \\ 2E_{13} &= \mathbf{a}_1 \cdot \mathbf{a}_3, \\ 2E_{23} &= \mathbf{a}_2 \cdot \mathbf{a}_3, \\ E_{33} &= 0. \end{aligned} \tag{6}$$

The current covariant base vectors of the mid-surface can be constructed by

$$\mathbf{a}_\alpha = \mathbf{r}_{,\alpha} = \mathbf{R}_{,\alpha} + \mathbf{v}_{,\alpha} = \mathbf{A}_\alpha + \mathbf{v}_{,\alpha}. \tag{7}$$

While constant parts of $E_{\alpha\beta}$ represent membrane strains, the parts linear in ξ^3 represent curvatures. $E_{\alpha 3}$ are the shear strains, which vanish in the case of shear rigid formulations, in which the current director $\mathbf{a}_3$ is orthogonal to the in-plane base vectors $\mathbf{a}_\alpha$.

2.2 | Hierarchic shell formulation with linearized transverse shear parametrization

The shear rigid Kirchhoff–Love (KL) shell formulation with nonlinear kinematics, which serves as a basis for our hierarchic shear deformable shell in Oesterle et al.,[19] describes the director in the current configuration as the current normal, using the in-plane base vectors

$$\mathbf{a}_3^{\mathrm{KL}} = \frac{\mathbf{a}_1 \times \mathbf{a}_2}{\|\mathbf{a}_1 \times \mathbf{a}_2\|} = \mathbf{a}_3^\perp. \tag{8}$$

From the orthogonality of the normal and the in-plane base vectors $\mathbf{a}_\alpha \cdot \mathbf{a}_3^\perp = 0$, it follows by differentiation w.r.t. ξ^β that a derivative of the normal can be moved to the in-plane basis:

$$\mathbf{a}_\alpha \cdot \mathbf{a}_{3,\beta}^\perp = -\mathbf{a}_{\alpha,\beta} \cdot \mathbf{a}_3^\perp. \tag{9}$$

Using the identity

$$\mathbf{a}_{\alpha,\beta} = \mathbf{a}_{\beta,\alpha}, \tag{10}$$

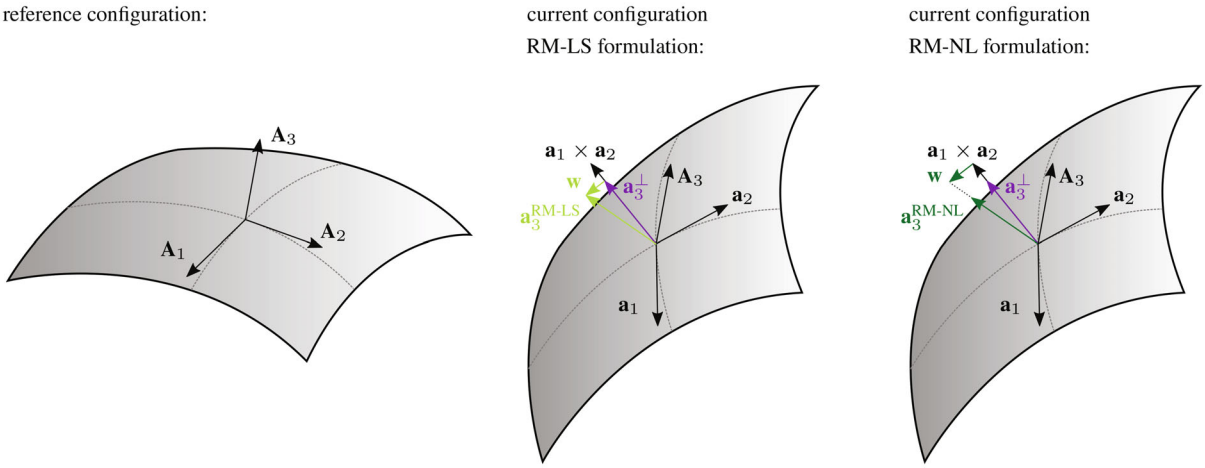

FIGURE 2 Mid-surface of the shell in reference configuration and current configurations for hierarchic shear deformable shell formulations with different shear parametrizations.

which follows from differentiation of the definition in Equation (7) w.r.t. ξ^β, the strain components for the Kirchhoff–Love formulation simplify to

$$\begin{aligned} E_{11}^{\mathrm{KL}} &= \mathbf{v}_{,1}\cdot\mathbf{A}_1 + \frac{1}{2}\mathbf{v}_{,1}\cdot\mathbf{v}_{,1} - \xi^3\left(\mathbf{a}_{1,1}\cdot\mathbf{a}_3^{\mathrm{KL}} - \mathbf{A}_{1,1}\cdot\mathbf{A}_3\right), \\ 2E_{12}^{\mathrm{KL}} &= \mathbf{v}_{,1}\cdot\mathbf{A}_2 + \mathbf{v}_{,2}\cdot\mathbf{A}_1 + \mathbf{v}_{,1}\cdot\mathbf{v}_{,2} - \xi^3 2\left(\mathbf{a}_{1,2}\cdot\mathbf{a}_3^{\mathrm{KL}} - \mathbf{A}_{1,2}\cdot\mathbf{A}_3\right), \\ E_{22}^{\mathrm{KL}} &= \mathbf{v}_{,2}\cdot\mathbf{A}_2 + \frac{1}{2}\mathbf{v}_{,2}\cdot\mathbf{v}_{,2} - \xi^3\left(\mathbf{a}_{2,2}\cdot\mathbf{a}_3^{\mathrm{KL}} - \mathbf{A}_{2,2}\cdot\mathbf{A}_3\right). \end{aligned} \tag{11}$$

For our geometrically nonlinear shear deformable Reissner–Mindlin shell formulation with linearized transverse shear parametrization[19] (RM-LS), the director is constructed in a hierarchic manner, by superimposing shear in form of a shear difference vector $\mathbf{w}$ to the deformed normal, compare Figure 2:

$$\mathbf{a}_3^{\mathrm{RM\text{-}LS}} = \frac{\mathbf{a}_1\times\mathbf{a}_2}{\|\mathbf{a}_1\times\mathbf{a}_2\|} + \mathbf{w} = \mathbf{a}_3^{\perp} + \mathbf{w}. \tag{12}$$

This construction technically violates the inextensibility condition $\|\mathbf{A}_3\| = \|\mathbf{a}_3\|$, since solely $\mathbf{a}_3^{\perp}$ is normalized, that is, only $\|\mathbf{A}_3\| = \|\mathbf{a}_3^{\perp}\|$ holds. However, the hypothesis in Oesterle et al.[19] is that in many problems shear rotations are relatively small compared to total rotations. Thus, the idea is to consider shear rotations in a linearized way, while bending and membrane parts of the deformation can be large, that is, they fully include geometrically nonlinear effects. A benefit of the proposed construction is that simplifications due to the orthogonality of $\mathbf{a}_\alpha$ and $\mathbf{a}_3^{\perp}$, that were made for the components of the strains in Equation (11), can be reused for this formulation. These membrane and bending related strain components are complemented by additional parts, responsible for transverse shear contributions. Consequently, the strain components show an additive structure:

$$\begin{aligned} E_{11}^{\mathrm{RM\text{-}LS}} &= \mathbf{v}_{,1}\cdot\mathbf{A}_1 + \frac{1}{2}\mathbf{v}_{,1}\cdot\mathbf{v}_{,1} - \xi^3\left(\mathbf{a}_{1,1}\cdot\mathbf{a}_3^{\perp} - \mathbf{A}_{1,1}\cdot\mathbf{A}_3\right) + \xi^3\left(\mathbf{w}_{,1}\cdot\mathbf{a}_1\right), \\ 2E_{12}^{\mathrm{RM\text{-}LS}} &= \mathbf{v}_{,1}\cdot\mathbf{A}_2 + \mathbf{v}_{,2}\cdot\mathbf{A}_1 + \mathbf{v}_{,1}\cdot\mathbf{v}_{,2} - \xi^3 2\left(\mathbf{a}_{1,2}\cdot\mathbf{a}_3^{\perp} - \mathbf{A}_{1,2}\cdot\mathbf{A}_3\right) + \xi^3\left(\mathbf{w}_{,1}\cdot\mathbf{a}_2 + \mathbf{w}_{,2}\cdot\mathbf{a}_1\right), \\ E_{22}^{\mathrm{RM\text{-}LS}} &= \mathbf{v}_{,2}\cdot\mathbf{A}_2 + \frac{1}{2}\mathbf{v}_{,2}\cdot\mathbf{v}_{,2} - \xi^3\left(\mathbf{a}_{2,2}\cdot\mathbf{a}_3^{\perp} - \mathbf{A}_{2,2}\cdot\mathbf{A}_3\right) + \xi^3\left(\mathbf{w}_{,2}\cdot\mathbf{a}_2\right), \\ 2E_{13}^{\mathrm{RM\text{-}LS}} &= \mathbf{a}_1\cdot\mathbf{w}, \\ 2E_{23}^{\mathrm{RM\text{-}LS}} &= \mathbf{a}_2\cdot\mathbf{w}. \end{aligned} \tag{13}$$

The additive structure of the strain components nicely visualizes the ability of this formulation to avoid transverse shear locking a priori, that is, before discretization, compare also Section 2.4. Furthermore, it is beneficial for the derivation of finite elements, as described in Section 2.5.

2.3 | Hierarchic shell formulation with nonlinear transverse shear parametrization

A fully nonlinear description of the director of the shear deformable Reissner–Mindlin formulation (RM-NL) using a difference vector is proposed by Long et al.,[12] compare Figure 2:

$$\mathbf{a}_3^{\text{RM-NL}} = \frac{\mathbf{a}_1 \times \mathbf{a}_2 + \mathbf{w}}{\|\mathbf{a}_1 \times \mathbf{a}_2 + \mathbf{w}\|}. \tag{14}$$

By normalization of the total director, the inextensibility condition is fulfilled, that is, $\|\mathbf{A}_3\| = \|\mathbf{a}_3^{\text{RM-NL}}\|$. However, the additive structure of the director is lost, and simplifications are impeded. The strain components remain similar to the ones described in Equation (6):

$$\begin{aligned}
E_{11}^{\text{RM-NL}} &= \mathbf{v}_{,1} \cdot \mathbf{A}_1 + \frac{1}{2}\mathbf{v}_{,1} \cdot \mathbf{v}_{,1} + \xi^3\left(\mathbf{a}_1 \cdot \mathbf{a}_{3,1}^{\text{RM-NL}} - \mathbf{A}_1 \cdot \mathbf{A}_{3,1}\right),\\
2E_{12}^{\text{RM-NL}} &= \mathbf{v}_{,1} \cdot \mathbf{A}_2 + \mathbf{v}_{,2} \cdot \mathbf{A}_1 + \mathbf{v}_{,1} \cdot \mathbf{v}_{,2} + \xi^3\left(\mathbf{a}_1 \cdot \mathbf{a}_{3,2}^{\text{RM-NL}} + \mathbf{a}_2 \cdot \mathbf{a}_{3,1}^{\text{RM-NL}} - \mathbf{A}_1 \cdot \mathbf{A}_{3,2} - \mathbf{A}_2 \cdot \mathbf{A}_{3,1}\right),\\
E_{22}^{\text{RM-NL}} &= \mathbf{v}_{,2} \cdot \mathbf{A}_2 + \frac{1}{2}\mathbf{v}_{,2} \cdot \mathbf{v}_{,2} + \xi^3\left(\mathbf{a}_2 \cdot \mathbf{a}_{3,2}^{\text{RM-NL}} - \mathbf{A}_2 \cdot \mathbf{A}_{3,2}\right),\\
2E_{13}^{\text{RM-NL}} &= \mathbf{a}_1 \cdot \mathbf{a}_3^{\text{RM-NL}},\\
2E_{23}^{\text{RM-NL}} &= \mathbf{a}_2 \cdot \mathbf{a}_3^{\text{RM-NL}}.
\end{aligned} \tag{15}$$

Although the director and the strain components do not show a purely additive structure, as opposed to Equations (12) and (13), the formulation is free from transverse shear locking, as explained in the following Section 2.4.

2.4 | Parametrization of the hierarchic shear difference vector

The shear difference vector for both linearized and nonlinear shear parametrization is constructed using the in-plane base vectors and the primary variables w^α, which are characterized as hierarchic rotations:

$$\mathbf{w} = w^1\mathbf{a}_1 + w^2\mathbf{a}_2. \tag{16}$$

For the RM-LS formulation, they are directly related to linearized shear angles, if the in-plane base vectors in Equation (16) are additionally normalized. For the RM-NL formulation, such geometrical relations for w^α are more cumbersome to establish, due to the non-additive construction of the director in Equation (14). With hierarchic rotations as distinct primary variables for transverse shear contributions at hand, it is obvious that bending deformations without transverse shear can easily be achieved (cf. Appendix A). Thus, in contrast to standard Reissner–Mindlin formulations, the hierarchic RM-LS and RM-NL formulations are intrinsically free from transverse shear locking, that is, transverse shear locking is avoided on formulation level instead of removing its effects after discretization on element level. However, as described in depth for the model problem of a Timoshenko beam in Oesterle et al.,[18] structural element formulations with hierarchic rotations still show an imbalance of function spaces in the kinematic equations for every equal order interpolation. While shear strains are fully balanced and, thus, shear locking is avoided, curvatures show different derivatives of the primary variables. The effect of this, herein called, *bending locking* in hierarchic rotation formulations for static analyses is that shear stress resultants still show some oscillations at the domain boundaries for low slenderness. Consequently, an alternative construction of the shear difference vector (16) was introduced in Oesterle et al.[18] and applied to large rotations in Oesterle et al.[19] It uses so called hierarchic displacements v^{s_α} instead of hierarchic rotations as primary variables. With these, the hierarchic rotation angles are described by derivatives of the hierarchic displacements $w^\alpha = v^{s_\alpha}_{,\alpha}$, which removes all imbalances from the kinematic equations and further improves the quality of stress resultants. However, since the RM-NL formulation of Long et al.[12] is originally parametrized by hierarchic rotations, we use the same for the RM-LS formulation to consistently compare the two formulations regarding the effects of linearized transverse shear.

2.5 | Derivation of element vectors and matrices

Thinking further in derivation of displacement based finite shell elements, the vector of internal element forces is built from the gradient of the strain energy, and the tangent stiffness matrix is the Hessian of the strain energy. Thus, first and

second derivatives of the strain components w.r.t. the five degrees of freedom u_r are needed: $(\,)_{,r} = \frac{\partial(\,)}{\partial u_r}$ and $(\,)_{,rs} = \frac{\partial^2(\,)}{\partial u_r \partial u_s}$ with $r = 1 \ldots 5$ and $s = 1 \ldots 5$. Due to the construction of the director or, respectively, the normal in Equations (8), (12), and (14), this involves the use of the quotient rule. Comparing the strain components in Equations (11), (13), and (15), it is seen that the RM-NL formulation is the only one that needs derivatives of a quotient at this stage. So, while for KL and RM-LS formulations the highest needed derivative of the director or, respectively, of the normal, is $\mathbf{a}^{\perp}_{3,r,s}$, which then already consists of five quotients (cf. eq. (5.32) in Kiendl[26]), the RM-NL formulation needs one further derivative $\mathbf{a}^{\text{RM-NL}}_{3,\alpha,r,s}$. Therefore, manual derivation of the element vectors and matrices is more complex and error-prone for the RM-NL formulation. As an alternative, automatic differentiation can be used, as recently done by Oberbichler et al.[27] or Vigliotti and Auricchio[28] for other elements.

3 | NUMERICAL STUDIES

3.1 | Overview

In this section, we investigate three geometrically nonlinear shell problems in order to study the effect of transverse shear deformation on the structural behavior. In particular, we scrutinize the assumption of small shear rotations. In the following, the shear deformable Reissner–Mindlin shell element with linearized transverse shear parametrization is denoted as RM-LS (in Oesterle et al.[19] this element is found with the abbreviation RM-hr). The newly implemented, geometrically fully nonlinear Reissner–Mindlin shell element on the basis of Long et al.[12] is abbreviated as RM-NL. To verify its correct implementation, we compare solutions to another fully nonlinear Reissner–Mindlin shell element RM-PBFE,[25] which is parametrized by total rotations, and which is available in our in-house research code Ikarus[29] ("PBFE" is for "projection based finite elements"). To contextualize any difference between the two shear deformable elements RM-LS and RM-NL, we add solutions for a shear rigid Kirchhoff–Love shell element (KL) on the basis of Kiendl et al.[11] Furthermore, in the third example we draw comparisons with 2D elements. All elements use NURBS-based shape functions and an equal order interpolation of all primary variables with polynomial degrees p and q for the two dimensions. All problems assume linear-elastic, isotropic material behavior using a St. Venant–Kirchhoff material law. The zero transverse normal stress condition $S^{33} = 0$, applied for Kirchhoff–Love and Reissner–Mindlin shell formulations, is incorporated into the material law as usual by elimination of the transverse normal strain E_{33} via static condensation. We compute internal force vectors and tangent stiffness matrices of the shear deformable elements RM-LS and RM-NL with automatic differentiation from the implemented strain energy using the C++ library autodiff.[30]

3.2 | Uniaxial bending

The first problem examines uniaxial bending of a beam-like structure. The problem setup is shown in Figure 3.

We choose different thicknesses t, which result in different slenderness ratios $\frac{L}{t}$. In addition to $\frac{L}{t} = 10$ and $\frac{L}{t} = 100$ from Oesterle et al.,[19] we include a very thin beam with $\frac{L}{t} = 1000$ and a very thick beam with $\frac{L}{t} = 4$. For the latter, the

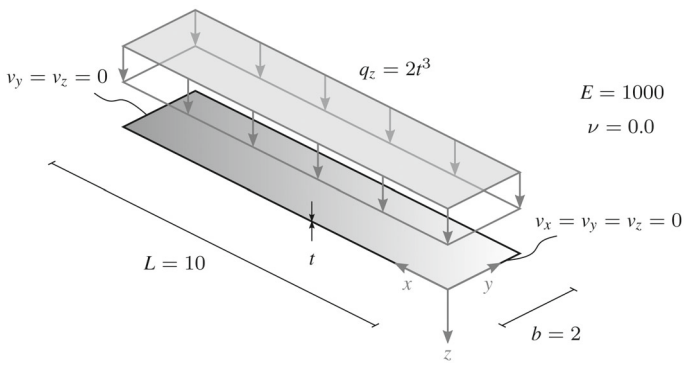

FIGURE 3 Uniaxial bending, problem setup.

TABLE 1 Uniaxial bending, maximum vertical displacement for various slenderness ratios.

Element	$\frac{L}{t} = 4$	$\frac{L}{t} = 10$	$\frac{L}{t} = 100$	$\frac{L}{t} = 1000$
KL	2.39820014	2.30316331	2.28637586	2.28620934
RM-LS	2.51315632	2.32381396	2.28658662	2.28621145
RM-NL	2.51799762	2.32394373	2.28658664	2.28621145
RM-PBFE	2.51799762	2.32394373	2.28658664	2.28621145

Note: Element names highlighted in color for better recognition.

ratio of the analytical solutions for the midpoint displacement by a Timoshenko beam theory w.r.t. Bernoulli beam theory is $\left(\left(\frac{L}{t}\right)^2 + 1.6\right)\left(\frac{L}{t}\right)^{-2} = 1.1$, so the difference between shear rigid and shear deformable theory in the geometrically linear case is 10%. For the given geometrically nonlinear case, containing the membrane deformation, which is not triggered in a linear analysis of this problem, this difference is expected to be smaller. However, the chosen statically determinate support keeps membrane effects as small as possible.

For all shell elements, sufficiently fine meshes are ensured with the help of mesh convergence studies. For this purpose, a variable number of cubic NURBS elements in x-direction is used for discretization, while in y-direction only one quadratic NURBS element is used. The mesh density is considered sufficient, if further refinement does not change the displacement solution with nine digits precision, as shown in Table 1. Effects from overstiff structural behavior due to transverse shear locking for the RM-PBFE element, bending locking for the RM-LS and RM-NL elements and membrane locking for all elements are thereby excluded. In x-direction the number of required elements is 80, 120, 160, or 200, depending on the type of shell element and the slenderness ratio. With 160 elements, the RM-PBFE element needs a finer mesh than RM-LS and RM-NL (80 elements) for the low slenderness ratio of 10. For the more slender geometry with $\frac{L}{t} = 100$, a coarser mesh with 80 elements is sufficient for RM-PBFE, while RM-LS and RM-NL need 120 and 160 elements. For the more extreme slenderness ratio values of 4 and 1000, the number of required elements is in the same range for all shell elements.

Table 1 shows the maximum vertical displacement for the various slenderness ratios. For the very thin beam, solutions of all shear deformable elements are in perfect agreement, since transverse shear deformations are practically insignificant for the displacement response. The identical results of RM-NL and RM-PBFE for all slenderness ratios verifies correct implementation of RM-NL. Comparing solutions of the KL element to all RM elements, it is seen that with lower slenderness ratios, that is, with larger thicknesses, transverse shear shows a greater influence on the solutions. The difference between shear rigid and shear deformable solutions for $\frac{L}{t} = 4$ with theoretically 10% for the linear case is reduced to 5% in the nonlinear setting here between KL and RM-NL elements. Compared to this, the difference between RM-LS and RM-NL with 0.2% for the very thick beam can be considered as negligible. Thus, in this range, linearization of transverse shear in the RM-LS formulation is legitimized by these results.

3.3 | Snap-through of a ring

The second problem deals with large total rotations. A closed ring is subject to a prescribed rotation about the z-axis at its top point while the bottom is fixed, so that after snap-through at a rotation of 2π, a deformed configuration with three overlapping rings results.[31] Figure 4 shows on the left a perspective view of the problem setup with the ring in y-z-plane and its width in x-direction. The concrete definition of the applied Dirichlet boundary conditions at the top and bottom control points is shown in Figure 4 on the right with a view onto the shell mid-surface, where the z-axis is placed at the shell boundary.

The ring is discretized by two patches with 50×1 elements each. In circumferential direction, a polynomial degree of $p = 3$ is chosen, whereas in width direction $q = 2$. Coupling of the two patches is realized using the bending-strip method.[32] Due to the pronounced imperfection sensitivity of this problem, the choice of stiffness for the bending strip crucially influences numerical stability of the iterative solution process. For the shear rigid KL element, the directional bending stiffness for the bending strip is set to $E_s = 5C^{11}$ with C^{11} being the entry of the linear-elastic material matrix $\mathbf{C}$ that relates curvature E_{11}^{lin} to stress S^{11} for the given material parameters. For the shear deformable elements RM-LS and RM-NL, directional bending stiffness is set to $E_s = 4C^{11}$. Different values may lead to solutions on secondary branches, which do not show symmetric snap-through but rather a lateral evasion of the ring.

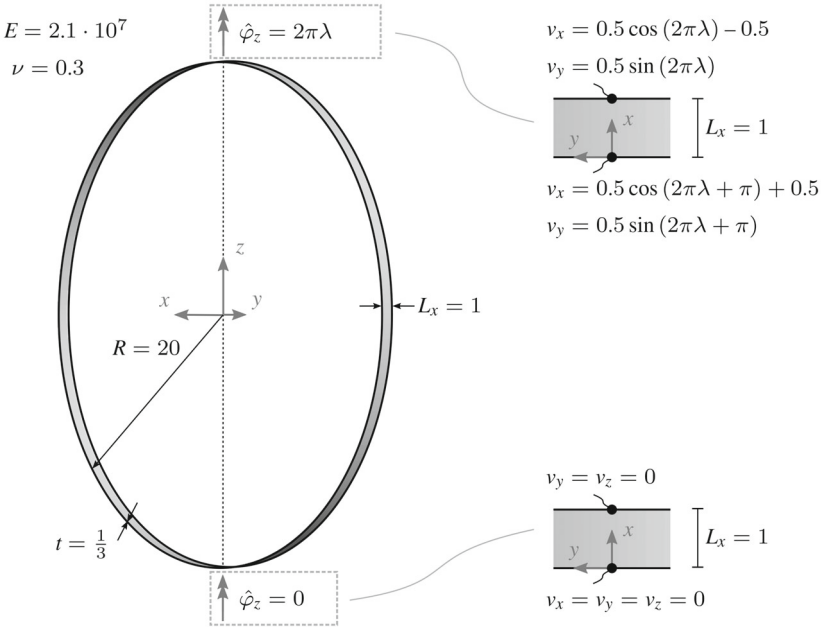

FIGURE 4 Snap-through of a ring, problem setup.

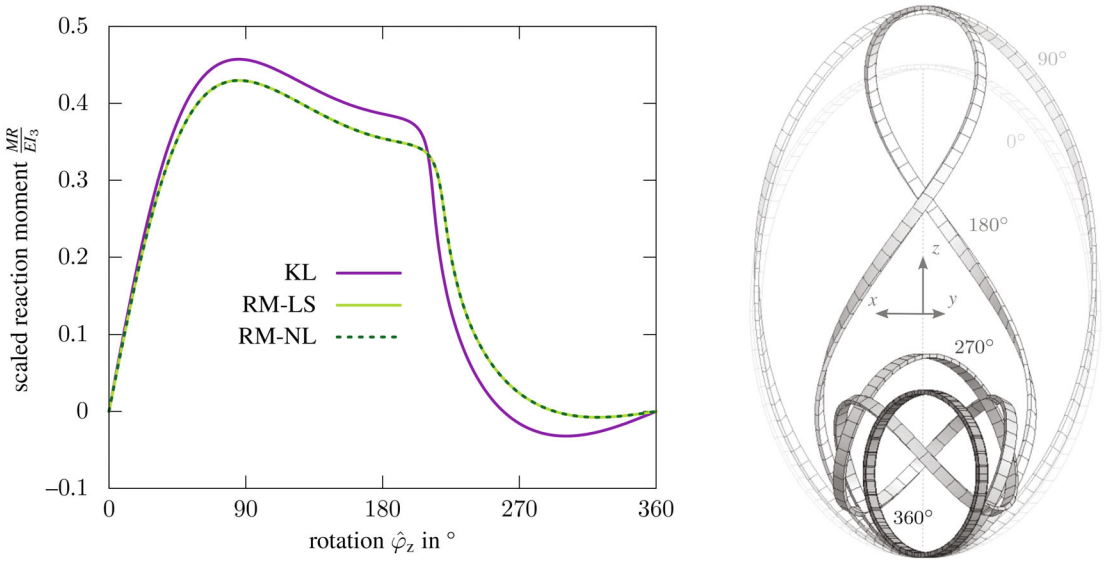

FIGURE 5 Snap-through of a ring, load-displacement diagram for scaled reaction moment over rotation angle (left) and five stages of the deformation process (right).

The load-displacement diagram in Figure 5 (left) shows the scaled reaction moment plotted versus the rotation angle $\hat{\varphi}_z$. The reaction moment M is calculated from the pair of reaction forces of the control points at the bottom. Its scaling $\frac{MR}{EI_3}$ with the ratio of radius to bending stiffness is taken from the literature, where this example is studied using beam elements. The value $EI_3 = \frac{1}{12}EtL_x^3$ describes the bending stiffness w.r.t. the axis in thickness direction θ^3. The difference between the solutions of KL and the shear deformable elements makes clear that considering transverse shear in this problem is relevant. We suspect that this difference is related to different ability of the models to represent the torsion of the beam-like structure. However, whether transverse shear is considered in a nonlinear manner or in a linearized manner, appears to be irrelevant here, as displayed by the perfectly coinciding solutions of RM-LS and RM-NL elements. Figure 5 (right) shows snapshots of the deformation process for five different angles of rotation.

3.4 | Simple shear

The motivation for the third problem is to trigger significant shear deformations. The idea is based on a flat shell with its upper bounding surface subject to horizontal static traction while the lower bounding surface is fixed to a rigid base, compare Figure 6.

Since the solution of the problem is homogeneous in x-direction, a discretization with one single shell element is sufficient. A representative element with in-plane dimensions $L_x = 2$ and $L_y = 2$, compare Figure 6, is chosen. The effect of static traction is applied by inhomogeneous Dirichlet boundary conditions on the shear degrees of freedom $w^1 = \hat{w}^1$ while all mid-surface displacement degrees of freedom are fixed, compare Figure 7 (left). Consequently, any cross-sectional rotation of the element is a pure shear rotation.

Figure 7 (right) shows the geometrical relation between the relative displacement u_{rel} between the upper and lower bounding surface of the shell and the rotation of the cross section φ_y. For the RM-LS element this geometrical relation is described by the tangent function, whereas for RM-NL it is the sine function. For a relative displacement of $u_{\text{rel}} \approx 0.6$, the solutions of RM-LS and RM-NL elements begin to significantly differ from each other. The assumption of linearization of transverse shear can therefore be assumed to be invalid for shear rotations larger than approximately 15°. However, in this deformation range, the underlying assumption of the Reissner–Mindlin shell model, namely cross-sectional fibers remaining straight during deformation, has to be questioned.

In order to study a possible warping of the cross section, we follow the concept of using a cubic ansatz in thickness direction, as it is used for a higher order 3D shell element in Willmann et al.[33] The problem is discretized by one single 2D NURBS element in the x-z-plane, using linear shape functions in x-direction and a cubic ansatz in z-direction. To isolate the warping effects from additional transverse strain effects (thickness change), inhomogeneous Dirichlet boundary conditions are applied in such a way that the cross-sectional length remains unchanged, compare Figure 8 (left). The deformation plot in Figure 8 (right) clearly shows the cross-sectional warping already for shear deformations smaller than $u_{\text{rel}} = 0.6$. Qualitatively similar results for the deformations can also be obtained by a discretization with bi-linear 2D elements when using multiple elements in z-direction. Hence, it can be concluded that during this deformation process

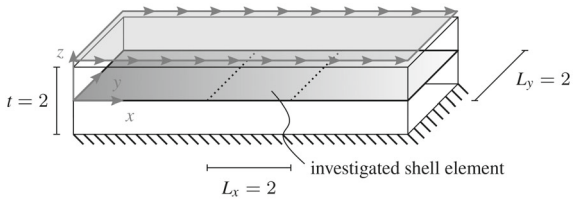

FIGURE 6 Simple shear, motivation.

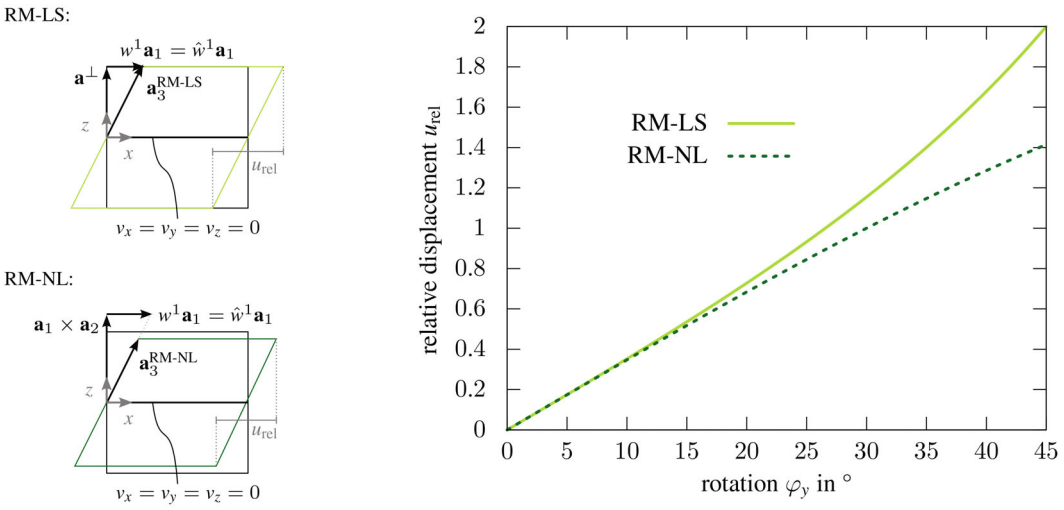

FIGURE 7 Simple shear, problem setup for shells (left) and relative displacement over cross-sectional rotation (right).

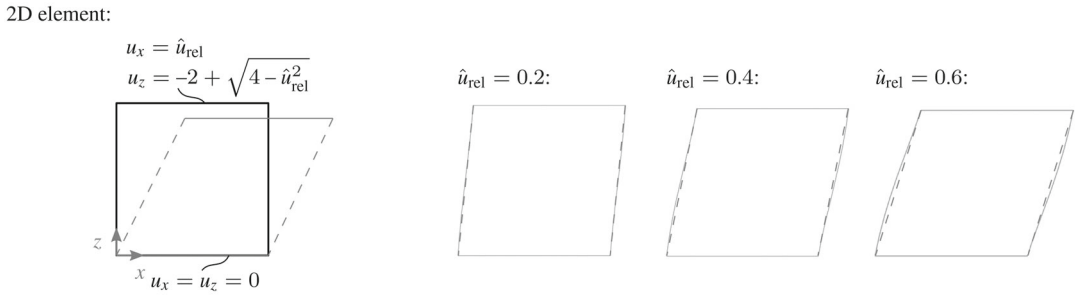

FIGURE 8 Simple shear, problem setup for 2D element (left) and deformations at various stages (right).

the basic assumption of straight cross sections becomes invalid *before* the assumption of linearized transverse shear leads to deviations from the three-dimensional solution. In other words: It does not seem to be sensible (or necessary) to take into account geometrical nonlinearity for transverse shear if at the same time the assumption of cross-sectional fibers remaining straight is maintained.

4 | CONCLUSIONS AND OUTLOOK

In this article, we critically questioned the assumption of small shear angles, which was made earlier for geometrically nonlinear hierarchic Reissner–Mindlin shell formulations in Oesterle et al. [19] This assumption leads to an additive split of strains in Equation (13), where parts related to shear deformation can be added to the strain components of a Kirchhoff–Love formulation. This simplifies the derivation of nonlinear finite shell elements compared to using a nonlinear representation of transverse shear. We have studied the effect of linearized transverse shear compared to nonlinear shear using NURBS based elements on the basis of *hierarchic rotation* formulations. We emphasize that the same conclusions hold for the *hierarchic displacement* Reissner–Mindlin formulation also derived in Oesterle et al.,[19] which also utilizes the assumption of linearized transverse shear.

For the numerical problem of uniaxial bending, we concluded that even for a very thick beam the influence of linearization of transverse shear is negligible when compared to the difference between shear deformable and shear rigid solutions. The problem of a ring snapping through showed that in a large total rotation problem, in which transverse shear deformations are in general relevant, there is no visible difference between solutions of the linearized transverse shear elements and the fully nonlinear ones. The simple shear problem, motivated by a static surface traction, showed that the assumption of linearized transverse shear is justified for problems with transverse shear deformations that are in a range where the assumption of cross-sectional fibers remaining straight during deformation is met.

In summary, we conclude that linearization of transverse shear strains in large rotation shell elements based on the Reissner–Mindlin model is a valid method.

When larger cross-sectional deformations evolve, which are in particular due to nonlinear constitutive behavior, for example, in large strain elasto-plasticity, further investigations are necessary extending the kinematics to shells with thickness changes, here named as *3D shells*, or to shells including cross-sectional warping, here named as *higher order 3D shells*, as presented for example by Willmann et al. [33] for sheet metal forming. Linearization of transverse shear inside a 3D shell formulation leads to a consequent continuation towards nonlinear kinematics of the hierarchic family of isogeometric shell finite elements, which was introduced in Echter et al.[14] for linear kinematics. The application of 3D shells or higher order 3D shells to laminated composites or sandwich structures with stiff outer layers and soft cores potentially gives also rise to large transverse shear deformations. Building on the results from the simple shear problem in Section 3.4, however, the authors assume that warping effects will be more relevant than the representation of nonlinear transverse shear also in these cases.

ACKNOWLEDGMENTS

The authors thank Tobias Willmann, Maximilian Schilling, and Alexander Müller for fruitful discussions on higher order shell elements and cross-sectional warping effects, as well as on finite shell elements in commercial software. This project is supported by the Deutsche Forschungsgemeinschaft (DFG, German Research Foundation) under Grant OE

728/1-1 – 428725889. This support is gratefully acknowledged. Open Access funding enabled and organized by Projekt DEAL.

DATA AVAILABILITY STATEMENT

The data that support the findings of this study are available from the corresponding author upon reasonable request.

ORCID

Rebecca Thierer https://orcid.org/0009-0008-0498-6053
Bastian Oesterle https://orcid.org/0000-0002-4505-0592
Manfred Bischoff https://orcid.org/0000-0003-1538-4281

REFERENCES

1. Reissner E. The effect of transverse shear deformation on the bending of elastic plates. *J Appl Mech*. 1945;12(2):A69-A77. doi:10.1115/1.4009435
2. Mindlin RD. Influence of rotatory inertia and shear on flexural motions of isotropic, elastic plates. *J Appl Mech*. 1951;18(1):31-38. doi:10.1115/1.4010217
3. Naghdi PM. The theory of shells and plates. In: Flügge S, ed. *Handbuch der Physik, Band 3/6a-2: Festkörpermechanik 2*. Springer; 1972.
4. Kirchhoff G. Über das Gleichgewicht und die Bewegung einer elastischen Scheibe. *J für Die Reine Und Angew Math*. 1850;1850(40):51-88. doi:10.1515/crll.1850.40.51
5. Love AEH. The small free vibrations and deformation of a thin elastic Shell. *Philos Trans R Soc Lond A*. 1888;179:491-546. doi:10.1098/rsta.1888.0016
6. Koiter WT. A consistent first approximation in the general theory of thin elastic shells. The Theory of Thin Elastic Shells; 1960:12-33.
7. Zienkiewicz OC, Taylor RL, Too JM. Reduced integration technique in general analysis of plates and shells. *Int J Numer Methods Eng*. 1971;3(2):275-290. doi:10.1002/nme.1620030211
8. Zienkiewicz OC, Taylor RL. *The Finite Element Method. Volume 2: Solid Mechanics*. Butterworth-Heinemann; 2000.
9. Zienkiewicz OC, Taylor RL, Fox DD. *The Finite Element Method for Solid and Structural Mechanics*. 7th ed. Elsevier/Butterworth-Heinemann; 2014.
10. Hughes TJR, Cottrell JA, Bazilevs Y. Isogeometric analysis: CAD, finite elements, NURBS, exact geometry and mesh refinement. *Comput Methods Appl Mech Eng*. 2005;194(39–41):4135-4195. doi:10.1016/j.cma.2004.10.008
11. Kiendl J, Bletzinger KU, Linhard J, Wüchner R. Isogeometric shell analysis with Kirchhoff–Love elements. *Comput Methods Appl Mech Eng*. 2009;198(49-52):3902-3914. doi:10.1016/j.cma.2009.08.013
12. Long Q, Bornemann PB, Cirak F. Shear-flexible subdivision shells. *Int J Numer Methods Eng*. 2012;90(13):1549-1577. doi:10.1002/nme.3368
13. Cirak F, Ortiz M, Schröder P. Subdivision surfaces: a new paradigm for thin-shell finite-element analysis. *Int J Numer Methods Eng*. 2000;47(12):2039-2072. doi:10.1002/(SICI)1097-0207(20000430)47:12¡2039::AID-NME872¿3.0.CO;2-1
14. Echter R, Oesterle B, Bischoff M. A hierarchic family of isogeometric shell finite elements. *Comput Methods Appl Mech Eng*. 2013;254:170-180. doi:10.1016/j.cma.2012.10.018
15. Auricchio F, Taylor RL. A shear deformable plate element with an exact thin limit. *Comput Methods Appl Mech Eng*. 1994;118(3):393-412. doi:10.1016/0045-7825(94)90009-4
16. Auricchio F, Taylor RL. A triangular thick plate finite element with an exact thin limit. *Finite Elem Anal Des*. 1995;19(1-2):57-68. doi:10.1016/0168-874X(94)00057-M
17. Bischoff M, Taylor RL. A three-dimensional shell element with an exact thin limit. In: Wasczyczyn Z, Pamin J, eds. *Proceedings of the 2nd European Conference on Computational Mechanics*. Fundacja Zdrowia Publicznego; 2001.
18. Oesterle B, Ramm E, Bischoff M. A shear deformable, rotation-free isogeometric shell formulation. *Comput Methods Appl Mech Eng*. 2016;307:235-255. doi:10.1016/j.cma.2016.04.015
19. Oesterle B, Sachse R, Ramm E, Bischoff M. Hierarchic isogeometric large rotation shell elements including linearized transverse shear parametrization. *Comput Methods Appl Mech Eng*. 2017;321:383-405. doi:10.1016/j.cma.2017.03.031
20. Neunteufel M, Schöberl J. The Hellan-Herrmann-Johnson and TDNNS method for linear and nonlinear shells. arXiv:2304.13806, 2023. doi:10.48550/arXiv.2304.13806
21. Oesterle B. *Intrinsisch Lockingfreie Schalenformulierungen*. PhD Thesis. Universität Stuttgart, Institut für Baustatik und Baudynamik; 2018. doi:10.18419/opus-10046
22. Belytschko T, Lin JI, Tsay CS. Explicit algorithms for the nonlinear dynamics of shells. *Comput Methods Appl Mech Eng*. 1984;42(2):225-251. doi:10.1016/0045-7825(84)90026-4
23. ANSYS Inc. LS-DYNA Theory Manual. Accessed October 12, 2023. https://ftp.lstc.com/anonymous/outgoing/web/ls-dyna&uscore;manuals/DRAFT/DRAFT&uscore;Theory.pdf
24. ANSYS Inc. SHELL181. Accessed October 12, 2023. https://www.mm.bme.hu/~gyebro/files/ans&uscore;help&uscore;v182/ans&uscore;elem/Hlp&uscore;E&uscore;SHELL181.html
25. Müller A, Bischoff M. A consistent finite element formulation of the geometrically non-linear Reissner-Mindlin Shell model. *Arch Comput Methods Eng*. 2022;30:3483. doi:10.1007/s11831-021-09702-7

26. Kiendl J. *Isogeometric Analysis and Shape Optimal Design of Shell Structures*. PhD Thesis. Technische Universität München, Lehrstuhl für Statik; 2011.
27. Oberbichler T, Wüchner R, Bletzinger KU. Efficient computation of nonlinear isogeometric elements using the Adjoint method and algorithmic differentiation. *Comput Methods Appl Mech Eng*. 2021;381:113817. doi:10.1016/j.cma.2021.113817
28. Vigliotti A, Auricchio F. Automatic differentiation for solid mechanics. *Arch Comput Methods Eng*. 2021;28(3):875-895. doi:10.1007/s11831-019-09396-y
29. Müller A, Mitruka VK, Mitruka TK. Ikarus v0.3. DaRUS; 2023. doi:10.18419/darus-3303
30. Leal AMM. Autodiff, a modern, fast and expressive C++ library for automatic differentiation. 2018. Accessed October 12, 2023. https://autodiff.github.io/
31. Yoshiaki G, Yasuhito W, Toshihiro K, Makoto O. Elastic buckling phenomenon applicable to deployable rings. *Int J Solids Struct*. 1992;29(7):893-909. doi:10.1016/0020-7683(92)90024-N
32. Kiendl J, Bazilevs Y, Hsu MC, Wüchner R, Bletzinger KU. The bending strip method for isogeometric analysis of Kirchhoff–Love shell structures comprised of multiple patches. *Comput Methods Appl Mech Eng*. 2010;199(37-40):2403-2416. doi:10.1016/j.cma.2010.03.029
33. Willmann T, Wessel A, Beier T, Butz A, Bischoff M. Cross-sectional warping in sheet metal forming simulations. *Proceedings of the 13th European LS-DYNA Conference*. DYNAmore GmbH; 2021.

How to cite this article: Thierer R, Oesterle B, Ramm E, Bischoff M. Transverse shear parametrization in hierarchic large rotation shell formulations. *Int J Numer Methods Eng*. 2024;125(9):e7443. doi: 10.1002/nme.7443

APPENDIX A. BENDING WITHOUT TRANSVERSE SHEAR

For vanishing primary transverse shear variables, that is, $w^1 = w^2 = 0$, the shear difference vector of Equation (16) vanishes as well:

$$\mathbf{w} = \mathbf{0}. \tag{A1}$$

For the RM-LS formulation, the Green–Lagrange strain components from Equation (13) reduce to

$$2E_{\alpha\beta}^{\text{RM-LS}} = \mathbf{v}_{,\alpha} \cdot \mathbf{A}_\beta + \mathbf{v}_{,\beta} \cdot \mathbf{A}_\alpha + \mathbf{v}_{,\alpha} \cdot \mathbf{v}_{,\beta} - \xi^3 2\left(\mathbf{a}_{\alpha,\beta} \cdot \mathbf{a}_3^\perp - \mathbf{A}_{\alpha,\beta} \cdot \mathbf{A}_3\right), \tag{A2}$$

which is recognized as the part of the KL formulation in Equation (11). With Equation (A1) it follows directly that the transverse shear strain components from Equation (13) vanish:

$$2E_{\alpha 3}^{\text{RM-LS}} = 0, \tag{A3}$$

which proves that the RM-LS formulation can display bending deformation without artificial transverse shear contributions.

For the RM-NL formulation, inserting Equation (A1) into the director definition of Equation (14) yields

$$\mathbf{a}_3^{\text{RM-NL}} = \mathbf{a}_3^\perp, \tag{A4}$$

showing that the RM-NL director reduces to the KL-type director from Equation (8). Inserting this into the Green–Lagrange strain components of Equation (15) gives:

$$2E_{\alpha\beta}^{\text{RM-NL}} = \mathbf{v}_{,\alpha} \cdot \mathbf{A}_\beta + \mathbf{v}_{,\beta} \cdot \mathbf{A}_\alpha + \mathbf{v}_{,\alpha} \cdot \mathbf{v}_{,\beta} + \xi^3 \left(\mathbf{a}_\alpha \cdot \mathbf{a}_{3,\beta}^\perp + \mathbf{a}_\beta \cdot \mathbf{a}_{3,\alpha}^\perp - \mathbf{A}_\alpha \cdot \mathbf{A}_{3,\beta} - \mathbf{A}_\beta \cdot \mathbf{A}_{3,\alpha}\right). \tag{A5}$$

According to Equations (9) and (10) the derivative can be shifted from the normal vector to the in-plane base vectors and symmetry holds. This results in simplified expressions for the Green–Lagrange strain components:

$$2E_{\alpha\beta}^{\text{RM-NL}} = \mathbf{v}_{,\alpha} \cdot \mathbf{A}_\beta + \mathbf{v}_{,\beta} \cdot \mathbf{A}_\alpha + \mathbf{v}_{,\alpha} \cdot \mathbf{v}_{,\beta} - \xi^3 2\left(\mathbf{a}_{\alpha,\beta} \cdot \mathbf{a}_3^\perp - \mathbf{A}_{\alpha,\beta} \cdot \mathbf{A}_3\right), \tag{A6}$$

which is, again, recognized as the part of the KL formulation from Equation (11), and

$$2E_{\alpha 3}^{\text{RM-NL}} = \mathbf{a}_\alpha \cdot \mathbf{a}_3^\perp = 0 \tag{A7}$$

holds due to orthogonality. As a consequence, bending deformations without transverse shear are possible as well with the RM-NL formulation.